

# Unilateral Multiple Facial Nerve Branch Reconstruction Using “End-to-side Loop Graft” Supercharged by Hypoglossal Nerve

Hajime Matsumine, MD,  
PhD\*†

Ryo Sasaki, DDS, PhD†‡

Yuichi Takeuchi, PhD§

Yorikatsu Watanabe, MD,  
PhD†

Yosuke Niimi, MD\*†

Hiroyuki Sakurai, MD, PhD\*

Mariko Miyata, MD, PhD§

Masayuki Yamato, PhD†

**Background:** Extensive facial nerve defects between the facial nerve trunk and its branches can be clinically reconstructed by incorporating double innervation into an end-to-side loop graft technique. This study developed a new animal model to evaluate the technique’s ability to promote nerve regeneration.

**Methods:** Rats were divided into the intact, nonsupercharge, and supercharge groups. Artificially created facial nerve defects were reconstructed with a nerve graft, which was end-to-end sutured from proximal facial nerve stump to the mandibular branch (nonsupercharge group), or with the graft of which other end was end-to-side sutured to the hypoglossal nerve (supercharge group). And they were evaluated after 30 weeks.

**Results:** Axonal diameter was significantly larger in the supercharge group than in the nonsupercharge group for the buccal ( $3.78 \pm 1.68$  vs  $3.16 \pm 1.22$ ;  $P < 0.0001$ ) and marginal mandibular branches ( $3.97 \pm 2.31$  vs  $3.46 \pm 1.57$ ;  $P < 0.0001$ ), but the diameter was significantly larger in the intact group for all branches except the temporal branch. In the supercharge group, compound muscle action potential amplitude was significantly higher than in the nonsupercharge group ( $4.18 \pm 1.49$  mV vs  $1.87 \pm 0.37$  mV;  $P < 0.0001$ ) and similar to that in the intact group ( $4.11 \pm 0.68$  mV). Retrograde labeling showed that the mimetic muscles were double-innervated by facial and hypoglossal nerve nuclei in the supercharge group.

**Conclusions:** Multiple facial nerve branch reconstruction with an end-to-side loop graft was able to achieve axonal distribution. Additionally, axonal supercharge from the hypoglossal nerve significantly improved outcomes. (*Plast Reconstr Surg Glob Open* 2014;2:e240; doi: 10.1097/GOX.0000000000000206; Published online 27 October 2014).

**R**econstruction of multiple facial nerve branches from a single facial nerve trunk is required after extensive loss of the facial nerve following the resections of malignant parotid tumors or

other surgical procedures. For treating facial nerve defects formed between the facial nerve trunk and its branches, cable grafting is used as a standard reconstruction procedure to transplant the multiple nerve

From the \*Department of Plastic and Reconstructive Surgery, Global Center of Excellence (COE) Program, Tokyo Women’s Medical University, Kawada-cho, Shinjuku-ku, Tokyo, Japan; †Institute of Advanced Biomedical Engineering and Science, Tokyo Women’s Medical University, Kawada-cho, Shinjuku-ku, Tokyo, Japan; ‡Department of Oral and Maxillofacial Surgery, Global Center of Excellence Program, Tokyo Women’s Medical University, Kawada-cho, Shinjuku-ku, Tokyo, Japan; and §Department of Physiology, School of Medicine, Tokyo Women’s Medical University, Kawada-cho, Shinjuku-ku, Tokyo, Japan.

Received for publication June 22, 2014; accepted September 4, 2014.

Copyright © 2014 The Authors. Published by Lippincott Williams & Wilkins on behalf of The American Society of Plastic Surgeons. *PRS Global Open* is a publication of the American Society of Plastic Surgeons. This is an open-access article distributed under the terms of the Creative Commons Attribution-NonCommercial-NoDerivatives 3.0 License, where it is permissible to download and share the work provided it is properly cited. The work cannot be changed in any way or used commercially.

DOI: 10.1097/GOX.0000000000000206

grafts between the trunk and reconstructed branches.<sup>1</sup> As a more efficient reconstruction technique in these cases, Kakibuchi et al<sup>2</sup> have reported “end-to-side loop graft,” a unique and innovative technique enabling surgeons to reconstruct multiple branches by an end-to-side suture allowing the distal stump of the facial nerve to be connected to the side wall of single transplanted nerve. The features of this technique include that (a) the reconstruction of multiple facial nerve branches can be achieved without an end-to-end suture to the proximal stump of the trunk of facial nerve using bundling nerve grafts and (b) shorter nerve grafts than that required for cable grafting are used, especially when many branches need to be reconstructed.<sup>2</sup> Using cross nerve grafts, Matsuda et al<sup>3</sup> have applied this technique to facial nerve reconstruction in a rat model and demonstrated that axonal distribution appears from the facial nerve trunk to 4 facial nerve branches, including 2 ipsilateral and 2 contralateral branches. On the other hand, axonal supercharge, a concept of actively inducing double innervation from multiple neural sources for more reliable functional recovery of the target organ, has recently been reported by several investigators.<sup>4-6</sup> Yamamoto et al<sup>5</sup> have performed an interpositional nerve graft involving 2 end-to-side sutures to transplant the greater auricular nerve between the facial nerve trunk and the hypoglossal nerve in patients with facial nerve palsy, and a strong muscle contraction is restored by establishing the double innervation of the mimetic muscles via the facial and hypoglossal nerves. To incorporate the concept of double innervation into the aforementioned end-to-side loop grafting, an end-to-side suture of the nerve end to the hypoglossal nerve can be made to create a network with multiple power sources that promote the distribution of more regenerating axons to each branch. This technique

contrasts with the original technique, which involves an end-to-end suture of the end of the nerve graft to the distal stump of the farthest facial nerve branch. However, many aspects of the end-to-side loop graft technique remain unknown, including (a) the quantity and percentage of axonal distribution to the 4 main branches of the facial nerve, (b) the localization of each branch in the facial nucleus, (c) the effect of axonal supercharge from the hypoglossal nerve enhanced by the function of the end-to-side loop graft, and (d) a question which branch is most benefited from the 4 branches over the axonal supercharge. These unknown factors are probably due to the lack of a suitable rat model for facial nerve reconstruction that precisely reproduces the original end-to-side loop graft technique used clinically, where a unilateral facial nerve trunk is used to reconstruct the 4 main ipsilateral facial nerve branches.

This study developed a new animal model for facial nerve reconstruction in rats to evaluate the combination of end-to-side loop graft technique for reconstructing the 4 main facial nerve branches using the ipsilateral facial nerve trunk with axonal supercharge from the hypoglossal nerve and physiologically and histologically evaluated the features of this technique and its ability to promote nerve regeneration.

## MATERIALS AND METHODS

### Surgical Procedure

Lewis rats (8 weeks old, approximately body weight: 200–250 g) were anesthetized with 4% isoflurane administered by a nasal mask<sup>7</sup> connected to a Univentor 400 Anesthesia Unit (Univentor, Zejtun, Malta). A preauricular incision with a marginal mandibular extension was made on the left side of the face to expose the trunk of facial nerve (TF), the temporal (TB), zygomatic, buccal (ZB), and marginal mandibular branches (MMB) of the facial nerve, and the hypoglossal nerve (HG) (Figs. 1A, B). The temporal, zygomatic, buccal, and marginal mandibular branches of the facial nerve were cut at the anterior border of the parotid gland using microsurgical scissors (MB-51-10; Natsume Seisakusho, Tokyo, Japan). The facial nerve trunk was cut at the inferior border of the auricular cartilage. The excised portion of the left facial nerve was then reconstructed by an end-to-side loop graft using a 20-mm autologous nerve graft taken from the contralateral buccal branch of the facial nerve.<sup>2</sup> The detailed procedure for nerve suturing was as follows. One end of the nerve graft was sutured to the facial nerve trunk by end-to-end neurorrhaphy, and the temporal, zygomatic, buccal, and marginal mandibular branches were sequentially su-

**Disclosure:** *The authors have no financial interest to declare in relation to the content of this article. This study was supported by the Formation of Innovation Center for Fusion of Advanced Technologies Project sponsored by the Special Coordination Funds for Promoting Science and Technology “Cell Sheet Tissue Engineering Center” and by the Global Center of Excellence Program at the Multidisciplinary Education and Research Center for Regenerative Medicine funded by the Ministry of Education, Culture, Sports, Science and Technology, Japan, as well as by the JST PRESTO program and Hiroto Yoshioka Memorial Fund for Medical Research. The Article Processing Charge was paid for by the authors.*

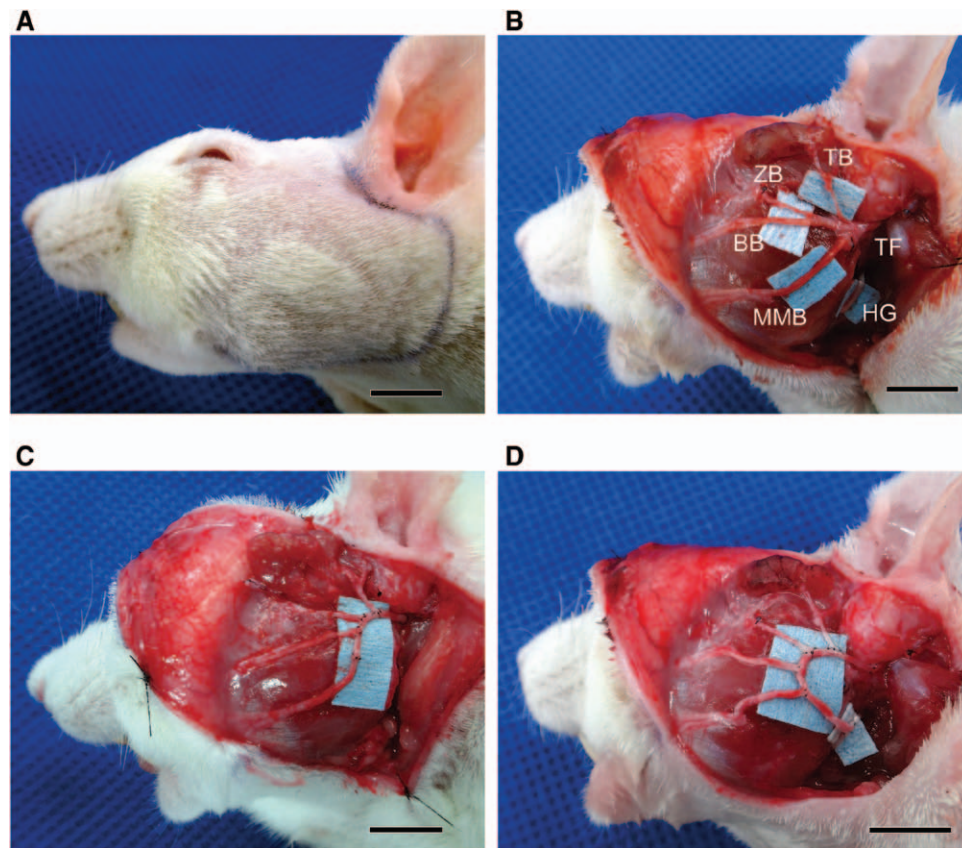


**Fig. 1.** Surgical procedure in a rat model. A, A preauricular incision with a marginal mandibular extension was made on the left side of the head. B, The trunk and 4 main branches of the facial nerve were exposed. BB indicates buccal branch of the facial nerve; HG, hypoglossal nerve; MMB, marginal mandibular branch of the facial nerve; TB, temporal branch of the facial nerve; TF, trunk of the facial nerve; ZB, zygomatic branch of the facial nerve. C, In the nonsupercharge group, each of the 4 branches was cut at the anterior border of the parotid gland and sutured to a nerve graft collected from the contralateral buccal branch of the facial nerve to make an end-to-side loop graft. D, In the supercharge group, the distal end of the transplanted nerve was end-to-side sutured to the hypoglossal nerve to obtain axonal supercharge. Scale bars show 10 mm.

tured by end-to-side neurorrhaphy at 2-mm intervals starting at a point 5 mm from the end-to-end suture of the facial nerve trunk (Fig. 1C). In the supercharge group, the other end of the nerve graft was end-to-side sutured to the hypoglossal nerve to obtain axonal supercharge (Fig. 1D). In the nonsupercharge group, the nerve graft was end-to-end sutured to the mandibular branch followed by cutting and removal of the excessive nerve graft (Fig. 1C). End-to-side sutures were performed through an epineural window, and all nerve sutures were performed by epineural suture using a 10-0 nylon suture (Nescosuture; Alfresa, Osaka) with a microscope (M651; Leica Microsystems, Wetzlar, Germany). Both transplanted (nonsupercharge and supercharge groups) and intact rats were subjected to histological and physiological evaluations at 30 weeks after transplantation. A 30-week period allowed the reconstructed

branches of facial nerve to mature sufficiently to show their physiologic functions such as compound muscle action potential (CMAP) safety.

All animal care and handling procedures were performed in accordance with the “Principles of Laboratory Animal Care” of Tokyo Women’s Medical University Animal Experimentation Committee.

#### Histological Analysis of Myelinated Fibers

The intact control and transplanted rats were deeply anesthetized with sodium pentobarbital and perfused with 4% paraformaldehyde solution via a cannula inserted into the left ventricle of the heart. After the trunk of facial nerve with the branches was removed, the temporal, zygomatic, buccal, and marginal mandibular branches of the facial nerve from the intact ( $n = 5$ ), nonsupercharge ( $n = 5$ ), and supercharge ( $n = 5$ ) groups (Figs. 2A–C) were

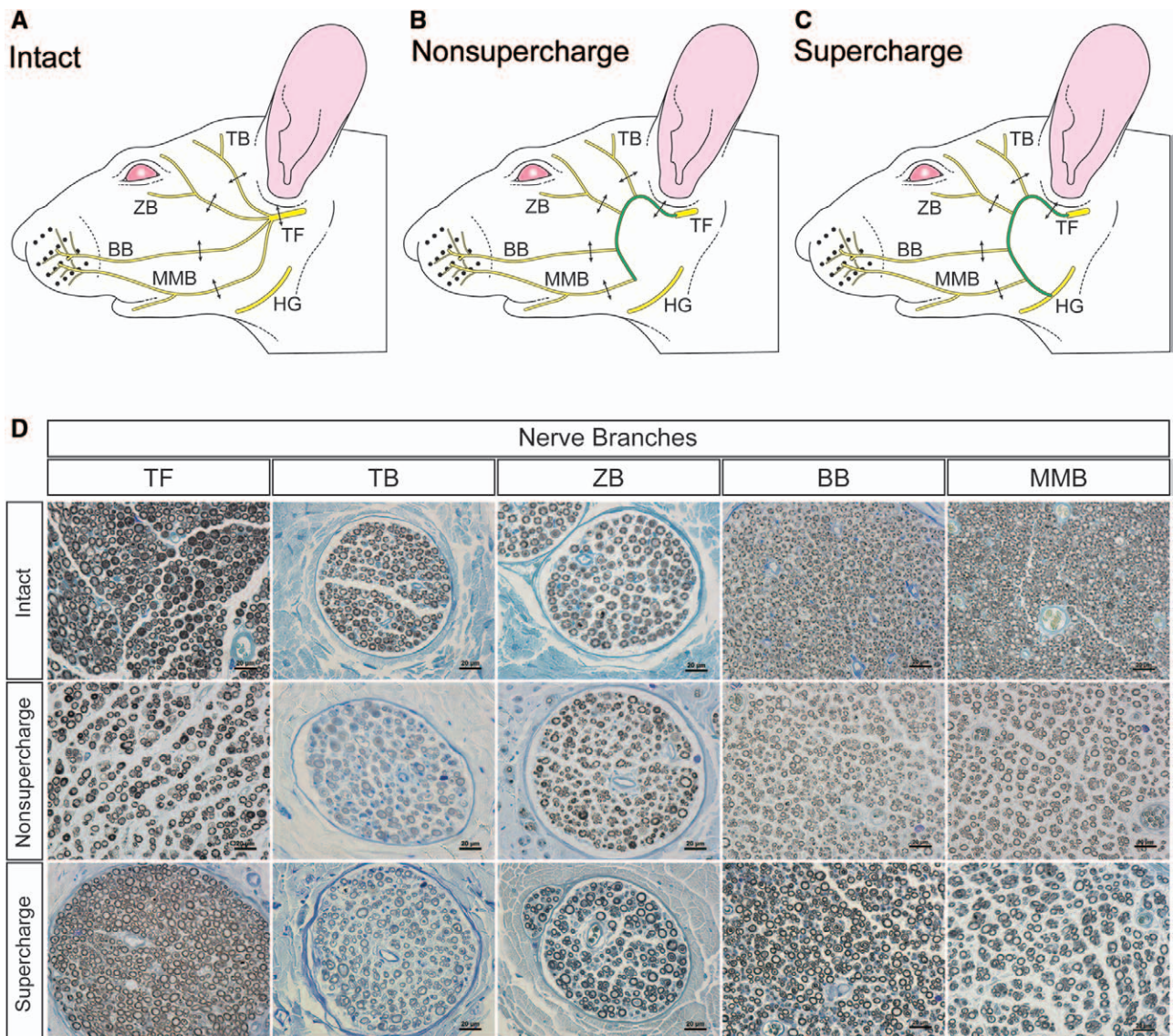


**Fig. 2.** Schematics of nerve collection sites in rat faces: the intact group (A); the nonsupercharge group (B); and the supercharge group (C). Double-ended arrows indicate the nerve collection sites. D, Osmium-toluidine blue staining of the cross section of the trunk of facial nerve and each branch in the intact, nonsupercharge, and supercharge groups. BB indicates buccal branch of the facial nerve; MMB, marginal mandibular branch of the facial nerve; TB, temporal branch of the facial nerve; TF, trunk of the facial nerve; ZB, zygomatic branch of the facial nerve. Scale bars shows 20  $\mu\text{m}$ .

fixed with 10% formalin in phosphate-buffered saline (PBS), postfixed in 1% osmium tetroxide for 10 days, dehydrated through a series of graded ethanols, and paraffin-embedded. Serial sections (1  $\mu\text{m}$  in thickness) were cut, stained with 0.1% toluidine blue, and examined with an Eclipse E800 light microscope (Nikon, Tokyo).

The myelinated fibers in each specimen ( $n = 15$ ) were manually counted by 2 examiners (twice each) under the light microscope, and the average was calculated (Fig. 2D). Axon diameter and myelin thickness were measured with ImageJ software version 1.47 (National Institutes of Health, Bethesda, Md.).

#### CMAP Recordings of the Vibrissal Muscles

CMAP was measured as described previously.<sup>8</sup> Briefly, rats were intraperitoneally anesthetized with urethane (1.2 g/kg body weight) and placed on a stereotaxic apparatus. Rectal temperature was maintained around 35–36 °C using a temperature controller (40-90-8D) (FHC, Bowdoin, Maine). Stages of anesthesia were maintained by confirming the lack of vibrissae movement and eyelid reflex.<sup>9</sup> To record CMAP, a stainless-steel microelectrode (9–12 M $\Omega$  at 1 kHz, UESMGCSELNMM-type) (FHC) was inserted into the vibrissal muscles between the middle vibrissal rows C and D. A reference electrode

(TN204-089B; Unique Medical, Tokyo) was placed caudally on the skull. To stimulate the reconstructed nerve, a tandem hook-shaped stimulation electrode (IMC-220224; Inter Medical, Aichi) was attached to the buccal branch of the facial nerve in the intact ( $n = 5$ ), nonsupercharge ( $n = 5$ ), and supercharge ( $n = 5$ ) groups, and monopolar stimulation pulses at a supramaximal level ( $\sim 2$  mA, 100  $\mu$ s) were delivered at 0.2 Hz via an isolator (SS-202J; Nihon Kohden, Tokyo). Recorded signals were processed with a multichannel amplifier (MEG-6100; Nihon Kohden) at 15–10,000 Hz and then digitized at 40 kHz using a PowerLab4/30 and LabChart7 system (ADInstruments, Dunedin, New Zealand). Data were analyzed in an offline manner with Igor Pro software (WaveMetrics, Lake Oswego, Ore.). The upward trace gave a negative deflection (depolarization), and 10 consecutive traces were averaged. Amplitude was measured as the difference in voltage between maximum and baseline CMAP amplitude. The duration of CMAP was calculated as the time between the 2 points where the baseline was crossed by the rising and declining CMAP curves.

#### Retrograde Labeling of Facial and Hypoglossal Motor Neurons through the Supercharged Nerve

Twenty-eight weeks after the surgery, rats were anesthetized with 4% isoflurane and injected, through a 25- $\mu$ L Hamilton syringe, with 200  $\mu$ L DiO (0.5%) in *N,N*-dimethylformamide (D-275) (Invitrogen, Carlsbad, Calif.) into the left whisker pad, 100  $\mu$ L DiI (1%) in ethanol (D-282) (Invitrogen) into the orbicularis oculi muscle, and 100  $\mu$ L DiD (1%) in ethanol (D-307) (Invitrogen) into the tongue. Two weeks later, rats were deeply anesthetized intraperitoneally with urethane or pentobarbital sodium and transcardially perfused with 150 mL physiological saline followed by 300 mL of 4% paraformaldehyde in 0.1 mol/L phosphate buffer (PB) at pH 7.4. The brain was then removed and postfixed overnight in the same fixative. Coronal sections (50  $\mu$ m in thickness) of the brain stem were made with a vibrating-blade microtome (VT1000S; Leica Microsystems), washed with 0.1 mol/L PB, mounted on gelatin-coated glass slides, and cover-slipped with an aqueous mounting medium. Images were taken by a Zeiss LSM 710 scanning confocal microscope with a 10 $\times$  objective

lens (Plan-Apochromat 10 $\times$ /0.45 M27) (Carl Zeiss, Oberkochen, Germany) with 0.7 $\times$  digital zoom.

#### Statistical Analysis

Results are expressed as the means  $\pm$  SD, and a probability value less than 0.05 was considered significant. The number of myelinated fibers, axon diameter, myelin thickness, CMAP amplitude, duration, and latency in each group were analyzed by analysis of variance and Tukey's multiple comparison test in GraphPad Prism version 6.00 for Windows (GraphPad Software, La Jolla, Calif.).

## RESULTS

Evaluation of postoperative facial appearance at 30 weeks after transplantation revealed that, in all rats in the nonsupercharge and supercharge groups, facial palsy was improved compared with immediately after reconstructive surgery, while the synkinesis of blinking and whisker movement were observed in all rats.

No significant differences were found in the number of myelinated fibers in the facial nerve trunk among the 3 groups. The numbers of myelinated fibers in the buccal and marginal mandibular branches in the nonsupercharge and supercharge groups were significantly higher than that in the intact group. No significant differences were observed between the nonsupercharge and supercharge groups in this parameter for any branches (Table 1 and Fig. 3A).

In terms of axon diameter, no significant differences were found in the trunk, temporal branch, and zygomatic branch of the facial nerve between the nonsupercharge and supercharge groups, whereas significantly larger diameters were noted in the supercharge group for the buccal and marginal mandibular branches—the 2 farthest branches from the trunk and the 2 closest branches to the hypoglossal nerve. Moreover, the diameter was significantly larger in the intact group than in the transplantation groups for all branches except the temporal branch (Table 2 and Fig. 3B).

With respect to myelin thickness, no significant differences were found in the trunk or temporal branch between the nonsupercharge and supercharge groups, whereas the supercharge group

**Table 1. Number of Myelinated Fibers of Reconstructed Branches of the Facial Nerve**

Group	Trunk of Facial Nerve	Temporal Branch	Zygomatic Branch	Buccal Branch	Marginal Mandibular Branch
Intact ( $n = 5$ )	3723 $\pm$ 725	217 $\pm$ 199	339 $\pm$ 64	1690 $\pm$ 176	1817 $\pm$ 284
Nonsupercharge ( $n = 5$ )	4470 $\pm$ 535	270 $\pm$ 145	554 $\pm$ 279	3714 $\pm$ 425	2991 $\pm$ 732
Supercharge ( $n = 5$ )	3815 $\pm$ 1262	336 $\pm$ 99	640 $\pm$ 169	3660 $\pm$ 582	3312 $\pm$ 246

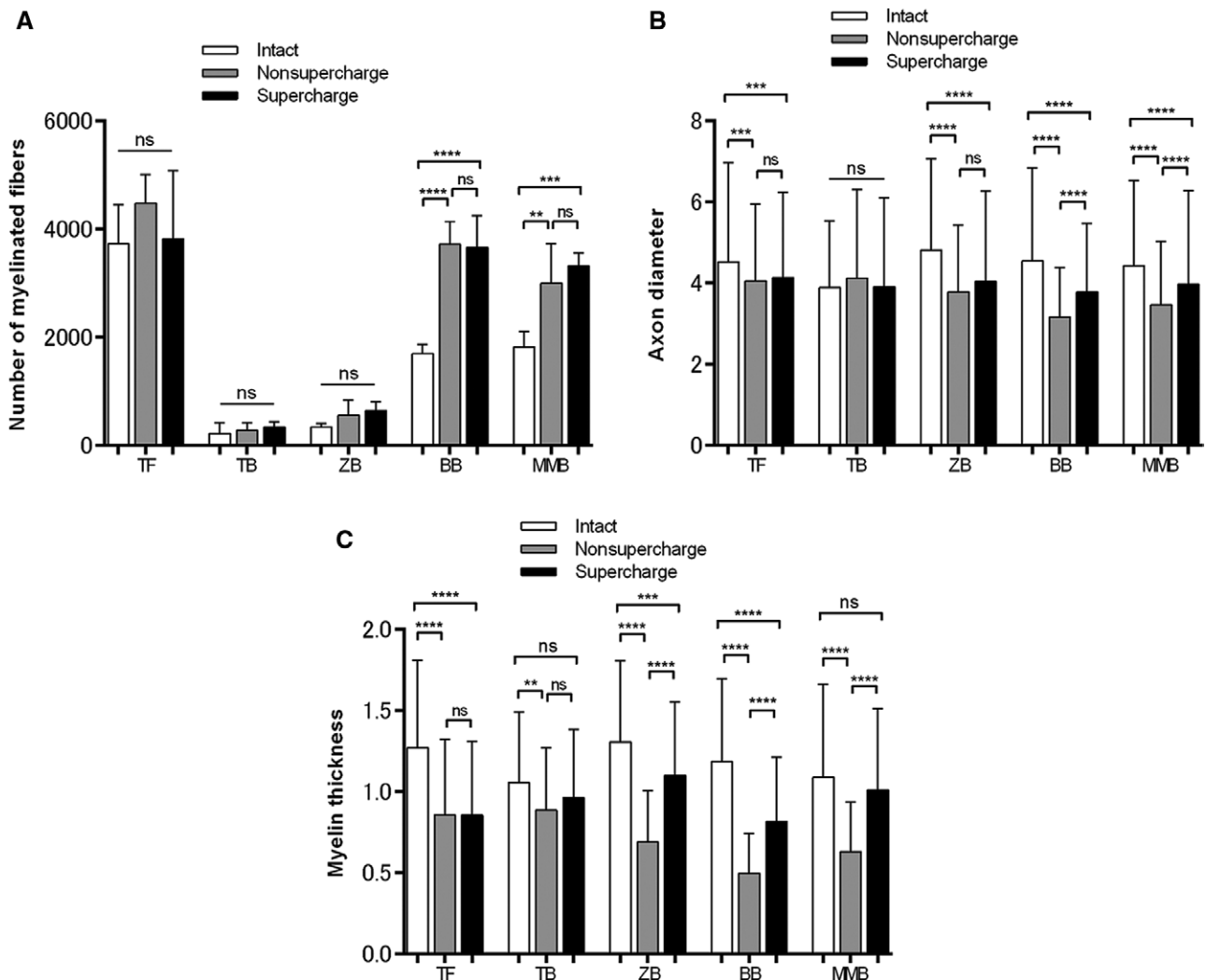


**Fig. 3.** The numbers of myelinated fibers, axon diameters, and myelin thicknesses of the intact, nonsupercharge, and supercharge groups. A, No significant differences were found in the numbers of myelinated fibers in the facial nerve trunk among the 3 groups. The numbers of myelinated fibers in the buccal and marginal mandibular branches in the nonsupercharge and supercharge groups were significantly higher than that in the intact group. No significant differences were found between the nonsupercharge and supercharge groups in this parameter for any branches. B, With respect to axon diameter, no significant differences were found between the nonsupercharge and supercharge groups for the trunk, temporal branch, or zygomatic branch of the facial nerve, whereas significantly higher values were noted in the supercharge group for the buccal and marginal mandibular branches compared with the nonsupercharge group. For all branches except for the temporal branch, the values in the intact group were significantly higher than those in the nonsupercharge and supercharge groups. C, With respect to myelin thickness, no significant differences were found between the nonsupercharge and supercharge groups for the trunk and temporal branch, whereas significantly higher values were noted in the supercharge group for the zygomatic, buccal, and marginal mandibular branches compared with the nonsupercharge group. For all branches, the values in the intact group were significantly higher than those in the nonsupercharge group. The values in the supercharge group were significantly lower than those in the intact group for the trunk, zygomatic branch, and buccal branch, whereas no significant differences were found for the temporal and marginal mandibular branches. BB indicates buccal branch; MMB, marginal mandibular branch of the facial nerve; TB, temporal branch; TF, trunk of the facial nerve; ZB, zygomatic branch. Analysis of variance and Tukey's multiple comparison test were used for statistical analyses. \*\* $P < 0.01$ ; \*\*\* $P < 0.001$ ; \*\*\*\* $P < 0.0001$ .

showed significantly thicker myelin for the other 3 branches away from the trunk (the zygomatic, buccal, and marginal mandibular branches) compared with the nonsupercharge group. All branches in the

intact group showed significantly thicker myelin than those in the nonsupercharge group. The values for the trunk, zygomatic branch, and buccal branch were significantly lower in the supercharge group

**Table 2. Axon Diameter of Reconstructed Branches of the Facial Nerve**

Group	Trunk of Facial Nerve ( $\mu\text{m}$ )	Temporal Branch ( $\mu\text{m}$ )	Zygomatic Branch ( $\mu\text{m}$ )	Buccal Branch ( $\mu\text{m}$ )	Marginal Mandibular Branch ( $\mu\text{m}$ )
Intact ( $n = 5$ )	4.52 $\pm$ 2.45	3.89 $\pm$ 1.64	4.81 $\pm$ 2.25	4.54 $\pm$ 2.30	4.42 $\pm$ 2.11
Nonsupercharge ( $n = 5$ )	4.04 $\pm$ 1.90	4.12 $\pm$ 2.18	3.78 $\pm$ 1.65	3.16 $\pm$ 1.22	3.46 $\pm$ 1.57
Supercharge ( $n = 5$ )	4.13 $\pm$ 2.11	3.90 $\pm$ 2.20	4.03 $\pm$ 2.23	3.78 $\pm$ 1.68	3.97 $\pm$ 2.31

**Table 3. Myelin Thickness of Reconstructed Branches of the Facial Nerve**

Group	Trunk of Facial Nerve ( $\mu\text{m}$ )	Temporal Branch ( $\mu\text{m}$ )	Zygomatic Branch ( $\mu\text{m}$ )	Buccal Branch ( $\mu\text{m}$ )	Marginal Mandibular Branch ( $\mu\text{m}$ )
Intact ( $n = 5$ )	1.27 $\pm$ 0.54	1.06 $\pm$ 0.43	1.31 $\pm$ 0.50	1.18 $\pm$ 0.51	1.09 $\pm$ 0.57
Nonsupercharge ( $n = 5$ )	0.86 $\pm$ 0.46	0.88 $\pm$ 0.38	0.69 $\pm$ 0.32	0.50 $\pm$ 0.25	0.63 $\pm$ 0.31
Supercharge ( $n = 5$ )	0.85 $\pm$ 0.45	0.96 $\pm$ 0.42	1.10 $\pm$ 0.45	0.82 $\pm$ 0.40	1.01 $\pm$ 0.50

than in the intact group, whereas no significant differences were found between the temporal and marginal mandibular branches (Table 3 and Fig. 3C).

In the physiological function evaluation by CMAP, the waveform of the supercharge group was more similar to that of the intact group than to that of the nonsupercharge group (Figs. 4A–C). CMAP amplitude in the supercharge group was significantly higher than that in the nonsupercharge group and similar to that in the intact group (Fig. 4D). No significant differences were found in CMAP duration among the 3 groups (Fig. 4E). With respect to CMAP latency, significantly better value was recorded in the intact group compared with the 2 transplanted groups, whereas no significant difference was found between the supercharge and nonsupercharge groups (Table 4 and Fig. 4F).

The fluorescent retrograde neuronal tracing analysis showed the distinct localization of DiI- or DiO-positive motor neurons innervating the orbicularis muscle and whisker pad in the facial nerve nucleus in the intact group (Fig. 5A). In the hypoglossal nerve nucleus, DiD-positive motor neurons were identified as the only positive innervating motor neurons (Fig. 5B). By contrast, in the nonsupercharge group, irregularly distributed motor neurons innervating the orbicularis muscle (DiI) and whisker pad (DiO) were observed in the facial nerve nucleus. In the hypoglossal nerve nucleus, consistent with that of the intact group, DiD-positive motor neurons were identified as the only positive innervating motor neurons (Fig. 5C). In the supercharge group, irregularly distributed motor neurons innervating the orbicularis muscle (DiI), whisker pad (DiO), and tongue (DiD) were observed in the facial nerve nucleus. These findings were similar to that observed in the hypoglossal nerve nucleus, with the irregular distribution of the motor neurons innervating the orbicularis muscle (DiI) and whisker pad (DiO) as well

as the tongue (DiD) (Fig. 5C). These results demonstrated that both mimetic muscles and tongue were double-innervated by the facial and hypoglossal nerve nuclei in the supercharge group.

## DISCUSSION

The results of the fluorescent retrograde neuronal tracing analysis and histology of nerve cross-sections showed that the end-to-side loop graft technique was able to achieve axonal distribution from the facial nerve trunk to its 4 branches (Fig. 6A). Moreover, the presence of bidirectional nerve regeneration in the transplanted nerves, as demonstrated by the coexistence of (a) axons extending from the mimetic muscles to the hypoglossal nerve nucleus and (b) axons extending from the tongue to the facial nerve nucleus, was achieved in the supercharge group (Fig. 6B). In the present experimental model using the end-to-side loop graft technique, the addition of supercharge from the hypoglossal nerve was associated with better nerve maturation, despite no significant difference in the numbers of axons, and better physiological results compared with the nonsupercharge group. There were 2 possible explanations for this. The first possible reason was the differential functions of the 2 motor sources: the facial nerve and the hypoglossal nerve. The hypoglossal nerve has notably stronger motor neurons than the facial nerve and can induce, therefore, the faster functional recovery of the facial mimetic muscles,<sup>10</sup> suggesting that these 2 nerves, despite having the same number of axons, were associated with the differential physiological performance of the mimetic muscles. This study assumed that in the physiological function test performed in this experimental model, the regenerating facial nerve branches containing axons originating from an additional motor source (the hypoglossal nucleus in the supercharge group) induced a stronger muscle contraction than

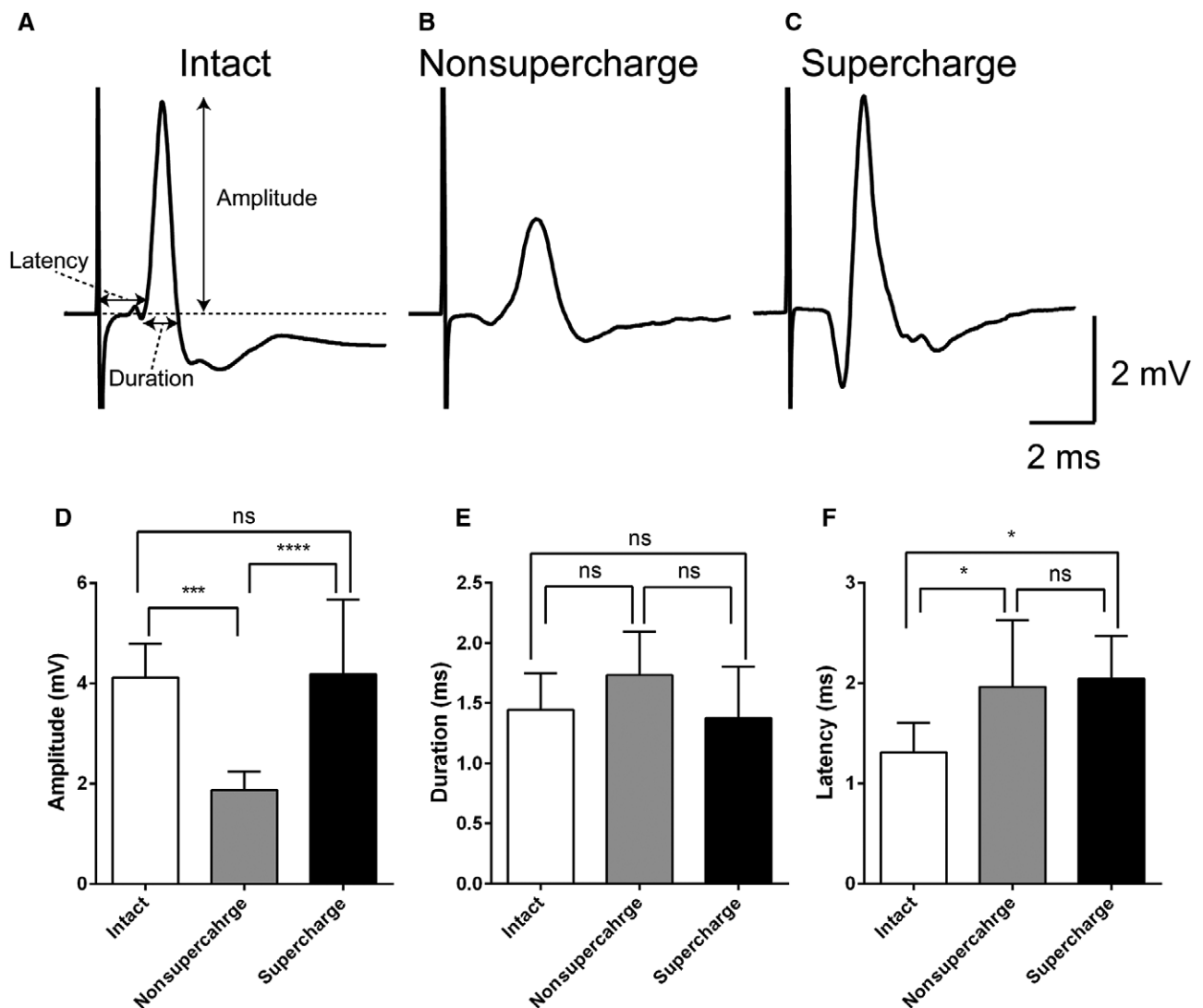


**Fig. 4.** Compound muscle action potential (CMAP) analysis. CMAPs recorded from a whisker pad after supramaximal stimulation in the intact (A), nonsupercharge (B), and supercharge (C) groups. Each trace was the mean of 10 consecutive raw traces. D, The mean CMAP amplitude was significantly higher in the supercharge group ( $4.18 \pm 1.49$  mV,  $n = 5$ ) than in the nonsupercharge group ( $1.87 \pm 0.37$  mV,  $n = 5$ ) and was similar to that in the intact group ( $4.11 \pm 0.68$  mV,  $n = 5$ ). E, No significant differences in CMAP duration among the intact ( $1.44 \pm 0.31$  ms), nonsupercharge ( $1.73 \pm 0.36$  ms), and control ( $1.38 \pm 0.43$  ms) groups were found. F, With respect to latency, significantly better values were recorded in the intact group ( $1.31 \pm 0.30$  ms) than the 2 transplanted groups, whereas no significant differences were found between the supercharge ( $2.04 \pm 0.43$  ms) and nonsupercharge ( $1.96 \pm 0.66$  ms) groups. Analysis of variance and Tukey's multiple comparison test were used for statistical analyses. \* $P < 0.05$ ; \*\*\* $P < 0.001$ ; \*\*\*\* $P < 0.0001$ .

**Table 4. Compound Muscle Action Potential of the Vibrissal Muscles**

Group	Amplitude (mV)	Duration (ms)	Latency (ms)
Intact ( $n = 5$ )	$4.11 \pm 0.68$	$1.44 \pm 0.31$	$1.31 \pm 0.30$
Nonsupercharge ( $n = 5$ )	$1.87 \pm 0.37$	$1.73 \pm 0.36$	$1.96 \pm 0.66$
Supercharge ( $n = 5$ )	$4.18 \pm 1.49$	$1.38 \pm 0.43$	$2.04 \pm 0.43$

those comprising only axons originating from the facial nerve nucleus (like the nonsupercharge group).

The second possible reason was that axonal supercharge allowed more axons to reach the mimetic mus-

cles within a shorter time, preventing the progressive deterioration of the target organ. The axon elongation rate is an important factor inhibiting collateral branching and terminal sprouting during nerve re-



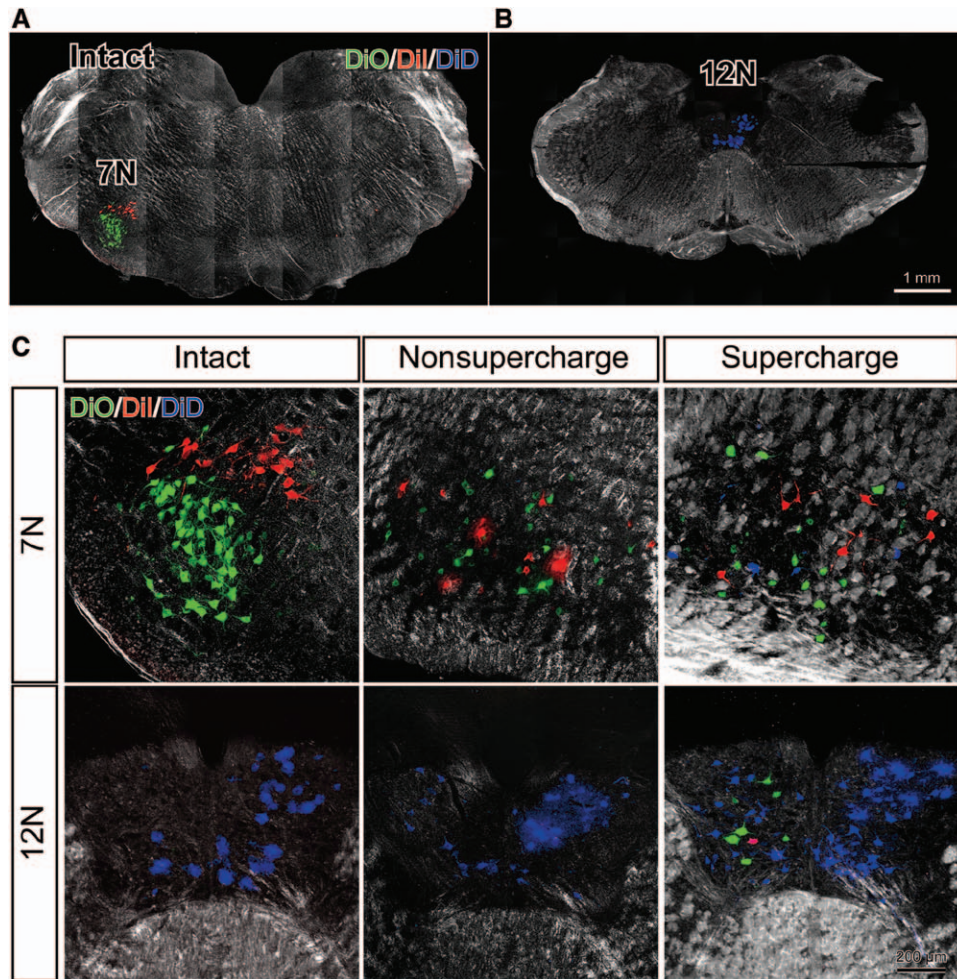


**Fig. 5.** Fluorescence retrograde neuronal tracing analysis with Dil, DiO, and DiD. The upper row shows the low-power coronal view of the rat brain stem. DiO- and Dil-labeled facial motor neurons (A) and DiD-labeled hypoglossal motor neurons (B) in intact rat facial and hypoglossal nuclei. Scale bar indicates 1 mm. C, High-power view of labeled facial and hypoglossal motor neurons in the intact, nonsupercharge, and supercharge groups. Scale bar indicates 200  $\mu\text{m}$ . Marks “7N” and “12N” indicate facial and hypoglossal nuclei, respectively.

generation.<sup>11</sup> The regeneration potentials of the 2 proximal branches of the facial nerve, the temporal and zygomatic branches, depended mainly on axonal elongation from the facial nerve nucleus, regardless of the presence of supercharge, meaning that the 2 branches had a similar axon elongation rate, resulting in similar histological findings in terms of regeneration. On the other hand, the 2 distal branches of the facial nerve, the buccal and marginal mandibular branches, received axon elongation from not only the facial nerve nucleus but also the hypoglossal nucleus, a more proximal motor source, in the presence of supercharge, meaning that more axons reached the target organ within a given time frame compared with the nonsupercharge group. Consequently, the branches closer to the hypoglossal nerve (ie, the motor source of axonal supercharge) more effectively

prevented the deterioration of the target organ and promoted nerve maturation.

This study also revealed several issues regarding the end-to-side loop graft technique. First, the technique, with or without supercharge, disrupted the myotrophic organization of the facial nerve branches. The loss of myotrophic organization might lead to the impaired physiological function of the mimetic muscles. Another issue was the possibility of collateral axonal branching caused by the technique. In this experimental model, although no significant differences were noted in the number of axons in the facial nerve trunk between the intact and end-to-side loop graft groups, the numbers of axons in all 4 branches were significantly higher than that of the latter group (Table 1). This was probably due to several collateral axonal branches originated from a single axon ex-

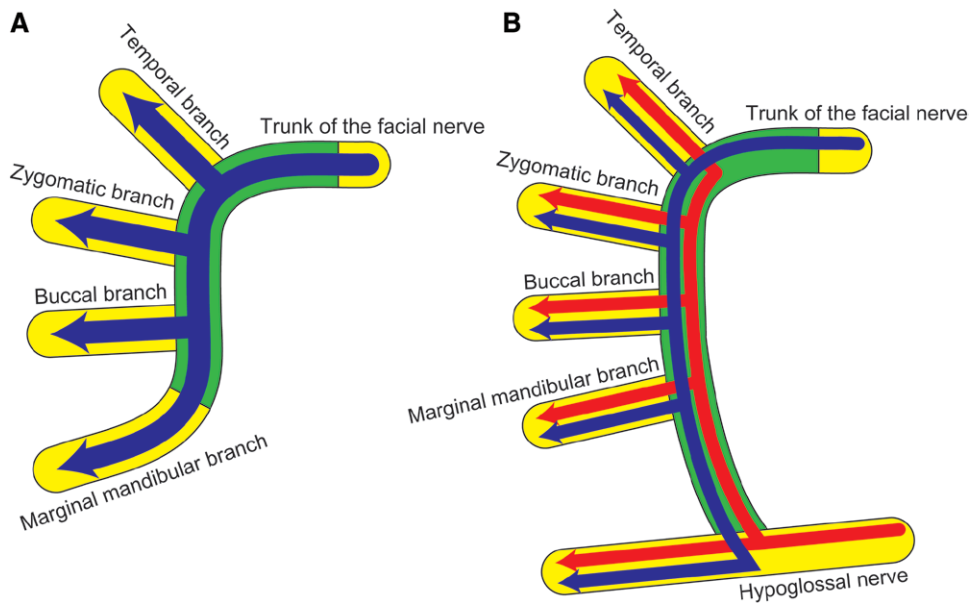


**Fig. 6.** Schemas of an end-to-side loop graft. A, The nonsupercharge model, and axonal distribution occurred from the trunk to the 4 branches of the facial nerve through the transplanted nerve. B, The supercharge model, and bidirectional axonal distribution occurred with axon elongation from both the facial nerve and hypoglossal nerve trunks. The yellow areas show the recipient nerve, and the green areas show the transplanted nerve. The blue arrows indicate axon elongation from the facial nerve trunk, and the red arrows indicate axon elongation from the hypoglossal nerve.

tending from the facial nerve nucleus in the end-to-side loop graft group. Collateral axonal branching at the lesion site and the regrowth of axons to incorrect muscles significantly delay the functional recovery of a regenerating facial nerve<sup>12</sup> and may also result in synkinesis. Both these factors were likely responsible for the inferior physiological function observed in the end-to-side loop graft group compared with the intact group. Therefore, additional strategies should be explored to promote a functional recovery after an end-to-side loop grafting.

The authors have previously reported that a vascularized nerve graft affords better nerve regeneration than a nonvascularized nerve graft in facial nerve reconstruction with a poorly neovascularized graft bed.<sup>8</sup> The authors expect that the combined use of a vascularized nerve graft with an end-to-side loop graft will lead to optimal functional recovery, which more closely resembles to what observed in the intact group than what obtained with the present experimental model.

### CONCLUSIONS

Unilateral multiple facial nerve branch reconstruction with an end-to-side loop graft was able to achieve reinnervation and axonal distribution. Although a level of nerve regeneration obtained by end-to-side loop grafting alone was lower than that

of the intact group, the addition of axonal supercharge from the hypoglossal nerve to end-to-side loop grafting significantly improved histological and physiological outcomes. The effect of axonal supercharge was more pronounced in branches closer to the hypoglossal nerve.

*Hajime Matsumine, MD, PhD*

Department of Plastic and Reconstructive Surgery  
 Institute of Advanced Biomedical  
 Engineering and Science  
 Tokyo Women's Medical University  
 8-1 Kawada-cho  
 Shinjuku-ku  
 Tokyo 162-8666  
 Japan  
 E-mail: matsumine@diary.ocn.ne.jp

### REFERENCES

1. May M, Schaitkin BM. History of facial nerve surgery. *Facial Plast Surg.* 2000;16:301-307.
2. Kakibuchi M, Tuji K, Fukuda K, et al. End-to-side nerve graft for facial nerve reconstruction. *Ann Plast Surg.* 2004;53:496-500.
3. Matsuda K, Kakibuchi M, Kubo T, et al. A new model of end-to-side nerve graft for multiple branch reconstruction: end-to-side cross-face nerve graft in rats. *J Plast Reconstr Aesthet Surg.* 2008;61:1357-1367.
4. Fujiwara T, Matsuda K, Kubo T, et al. Axonal supercharging technique using reverse end-to-side neuroorrhaphy in peripheral nerve repair: an experimental study in the rat model. *J Neurosurg.* 2007;107:821-829.

5. Yamamoto Y, Sekido M, Furukawa H, et al. Surgical rehabilitation of reversible facial palsy: facial–hypoglossal network system based on neural signal augmentation/neural supercharge concept. *J Plast Reconstr Aesthet Surg*. 2007;60:223–231.
6. Isaacs J, Allen D, Chen LE, et al. Reverse end-to-side neurotization. *J Reconstr Microsurg*. 2005;21:43–48; discussion 49–50.
7. Sasaki R, Matsumine H, Watanabe Y, et al. Anesthesia for research on reconstructive facial surgery in rats. *J Reconstr Microsurg*. 2013;29:209–210.
8. Matsumine H, Sasaki R, Takeuchi Y, et al. Vascularized versus nonvascularized island median nerve grafts in the facial nerve regeneration and functional recovery of rats for facial nerve reconstruction study. *J Reconstr Microsurg*. 2014;30:127–136.
9. Friedberg MH, Lee SM, Ebner FF. Modulation of receptive field properties of thalamic somatosensory neurons by the depth of anesthesia. *J Neurophysiol*. 1999;81:2243–2252.
10. Neiss WF, Guntinas Lichius O, Angelov DN, et al. The hypoglossal-facial anastomosis as model of neuronal plasticity in the rat. *Ann Anat*. 1992;174:419–433.
11. Guntinas-Lichius O, Hundeshagen G, Paling T, et al. Impact of different types of facial nerve reconstruction on the recovery of motor function: an experimental study in adult rats. *Neurosurgery* 2007;61:1276–1283; discussion 1283–1285.
12. Guntinas-Lichius O, Irintchev A, Streppel M, et al. Factors limiting motor recovery after facial nerve transection in the rat: combined structural and functional analyses. *Eur J Neurosci*. 2005;21:391–402.